Fabrication of collagen films with enhanced mechanical and enzymatic stability through thermal treatment in fluorous media

*Lan Zhang [1, 2, ‡], Sanjana Gopalakrishnan[1, ‡], Kai Li[2], Li-sheng Wang[1], Yong Han[2, *], Vincent M. Rotello[1,*]*

1 Department of Chemistry, University of Massachusetts Amherst, MA, 01003, USA

2 State-key Laboratory for Mechanical Behavior of Materials, Xi'an Jiaotong University, Xi'an 710049, China

KEYWORDS Collagen I, stability, mechanical properties, thermal treatment, biomaterials

ABSTRACT

Collagen I (Col-I) is widely used in the fabrication of biomaterials due to its biocompatibility, however Col-I based biomaterials are susceptible to mechanical failure during handling, which limits their applicability to biomaterials. Chemical or physical treatment can improve the mechanical properties of collagen however, these processes can create issues of cytotoxicity or denaturation. We report here an alternative strategy to improve the stability and mechanical properties of Col-I while preserving its native structure, through thermal treatment in fluorous media. Thermal treatment of Col-I in fluorous solvent generates compact, stable films with significantly increased mechanical strength. Furthermore, the use of fluorous media significantly reduces the extent of swelling, rate of proteolytic degradation, and preserves the high cell biocompatibility.

INTRODUCTION

Collagen I (Col-I) is the major component of the extracellular matrix in mammalian tissue.[1] The unique triple helix structure provides multiple cell attachment sites and plays an essential role in promoting cell behavior including adhesion, proliferation, migration and differentiation.[2] Col-I has been utilized as a biomaterial in several forms, such as injectable hydrogels,[3] sponges,[4] nanofibers,[5] hollow spheres,[6] and films[7]. Col-I based materials have been used in conjunction with biomaterial applications such as soft/ hard tissue repair strategies,[7] tissue engineering scaffolds,[8] and wound healing systems[9]. Furthermore, as collagen is a naturally derived protein, it enables sustainable fabrication of biomaterials.[10]

Collagen-based biomaterials often lack sufficient strength and stability, and are prone to both mechanical damage and rapid enzymatic digestion.[4] Several processes have been used to enhance the mechanical properties of collagen matrix. For instance, incorporating components such as graphene increases the stiffness of collagen-based matrix.[10, 11] However, this incorporation can jeopardize both the cytophilic properties and biocompatibility of the resulting materials. Crosslinking is a common way to modify collagen to enhance strength as well as improve enzymatic stability. [12] The usual methods of crosslinking are chemical and physical crosslinking.[1] Chemical cross-linkers (e.g. glutaraldehyde, carbodiimide) can reduce cytocompatibility because either the linkers themselves or the byproducts are cytotoxic.[12] Using a physical method such as dehydrothermal treatment or irradiation can avoid cytotoxicity from the added cross-linking agent. Thermal treatment in particular has been shown to induce crosslinking and tight packing of collagen fibers.[13, 14, 15] However, collagen tends to undergo uncontrolled denaturation during such treatments, unfavorably affecting materials properties.[16]

Perfluorocarbons provide an inert, stable environment due to their immiscibility with water as well as most organic solvents.[17, 18, 19] Furthermore, proteins in perfluorocarbon solvents are not prone to denaturation like proteins in organic solvents.[20] We have previously demonstrated our ability to stabilize protein films from aqueous degradation through thermal treatment in a fluorous media (perfluoroperhydrophenanthrene, PFHP), chosen for its high boiling point (216°C) and ready availability. We also showed that the native secondary structures and surface properties of the proteins are retained after treatment in PFHP.[21] Therefore, we hypothesized that the stability and mechanical properties of the Col-I matrix could be improved by thermal treatment in PFHP, *without* compromising the protein structure. We report here the use of fluorous thermal treatment to improve both the mechanical and biostability of collagen films. In this study, the stability and mechanical properties of Col-I were evaluated after thermal treatment in PFHP and compared to as-prepared Col-I and Col-I heat-treated in air **(Figure 1)**, with clear improvements in mechanical properties and enzymatic stability observed with fluorous treatment. Cytocompatibility was retained, as demonstrated through the incubation of fibroblast cells. Overall, thermal treatment in PHFP enhances both the stability and mechanical properties of Col-I while retaining cytocompatibility and preventing significant denaturation.

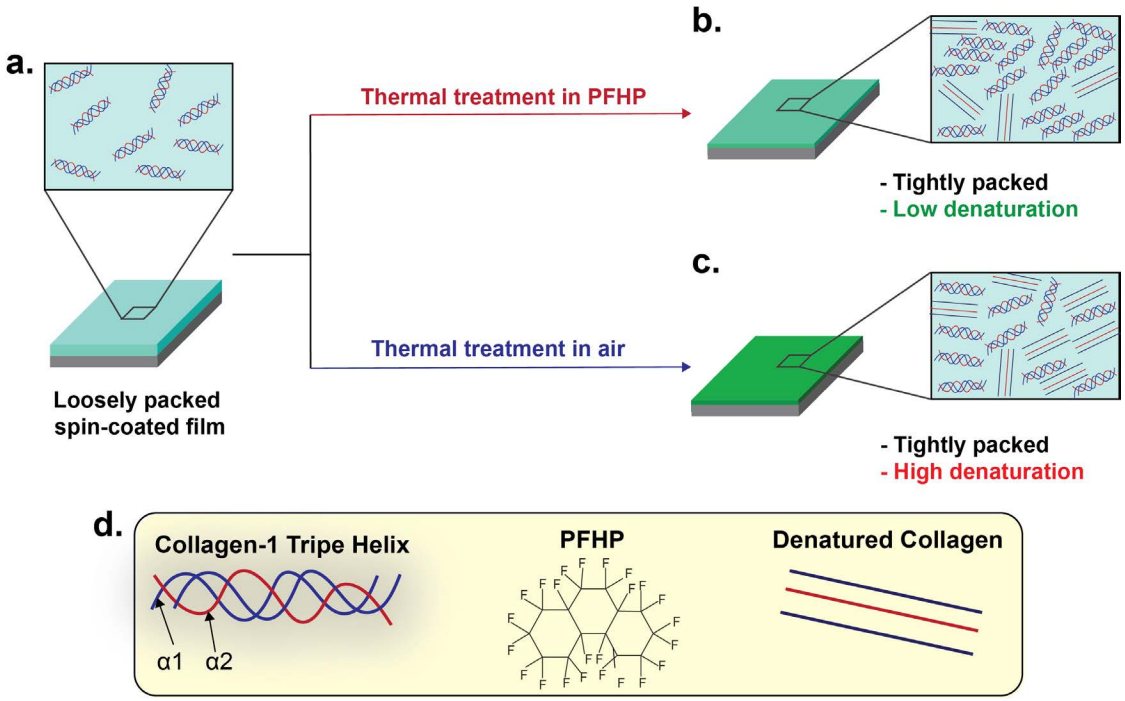

Figure 1. Schematic Representation of the fabrication strategy for stable collagen films. (a) Spin-coating of Col-I solution on cleaned silicon substrates produces films with loosely packed collagen fibers. (b) Low degree of denaturation of Col-I with fluorous heat treatment and (c) a high degree of denaturation after heat treatment in air. (d) Schematic showing representative structure of Col-I triple helix, PFHP and denatured col-I fibers

RESULTS AND DISCUSSION

The post-treatment surface topographies of collagen coatings prepared on Si wafers are shown in **Figure 2**. The SC (spin-coated) surface is smooth, with collagen covering the surface homogeneously, forming a net-like structure with an average roughness (R_a) of 0.48 nm **(Figure 2(a))**. Fluorous-cured (FC) or air-cured (AC) collagen films treated at 75, 135 and 180 °C showed no significant changes in roughness as compared to SC films **(Figures 2(b)-2(g))**. We therefore concluded that thermal treatment does not significantly affect the nano-topography of the surface. The surface morphologies observed by FESEM **(Figure S1)** are also in accordance with the AFM results indicated in **Figure 2**.

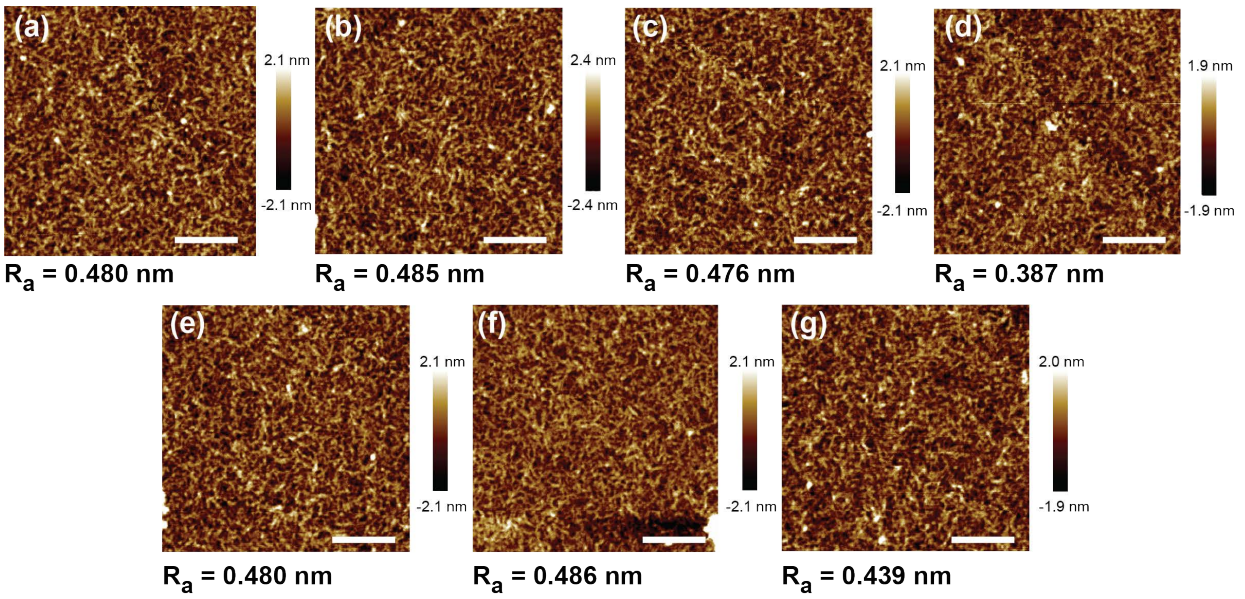

Figure 2. Surface-topographies of different coating surfaces imaged by AFM: (a) SC, (b)FC75 (c) FC135, (d)FC180, (e)AC75, (f)AC135, (g)AC180. Scale bar is 1 μm. Height profiles indicate surface roughness of each film. Roughness (R_a) of each sample is reported under the image. Thermal treatment does not significantly affect the nano-topography of the surface.

The thickness of different coatings as measured by ellipsometry are shown in **Figure 3(a)**. As the temperature is increased, the thickness of coating decreases, indicating tighter packing of the collagen fibers due to thermal treatment Additionally, there is no significant difference between FC films and AC films, which indicates that the fluorous treatment does not significantly affect the temperature-induced reorganization of the collagen fibers. The thickness of FC-180 obtained through the cross-sectional image obtained by FESEM as seen in **Figure 3(b)**, is in agreement with the ellipsometry measurements in **Figure 3(a)** (see also **Figure S2**). Thermal treatment of Col-I is known to induce reaction between two or more collagen molecules via carboxylic acids and amines, inducing intermolecular crosslinking without inducing cytotoxicity.[15] Furthermore, collagen chains shrink and pack tightly during thermal treatment.[15, 16]

Changes in the hydrophilicity of the collagen films due to thermal treatment was assessed through water contact angle measurements. As shown in **Figure 3(c)**, Fluorous-cured films (FC75, FC135 and FC180) have increased contact angles as compared to the spin-cast (SC) film (by ~30°) and air-cured

films (AC75, AC135 and AC180). This change in contact angle indicates that there is a difference in the reorganization behavior of collagen fibers during both treatments. We hypothesized that PFHP treatment results in tighter packing of collagen fibers than air curing, contributing to lower wettability and therefore a greater increase in contact angles.

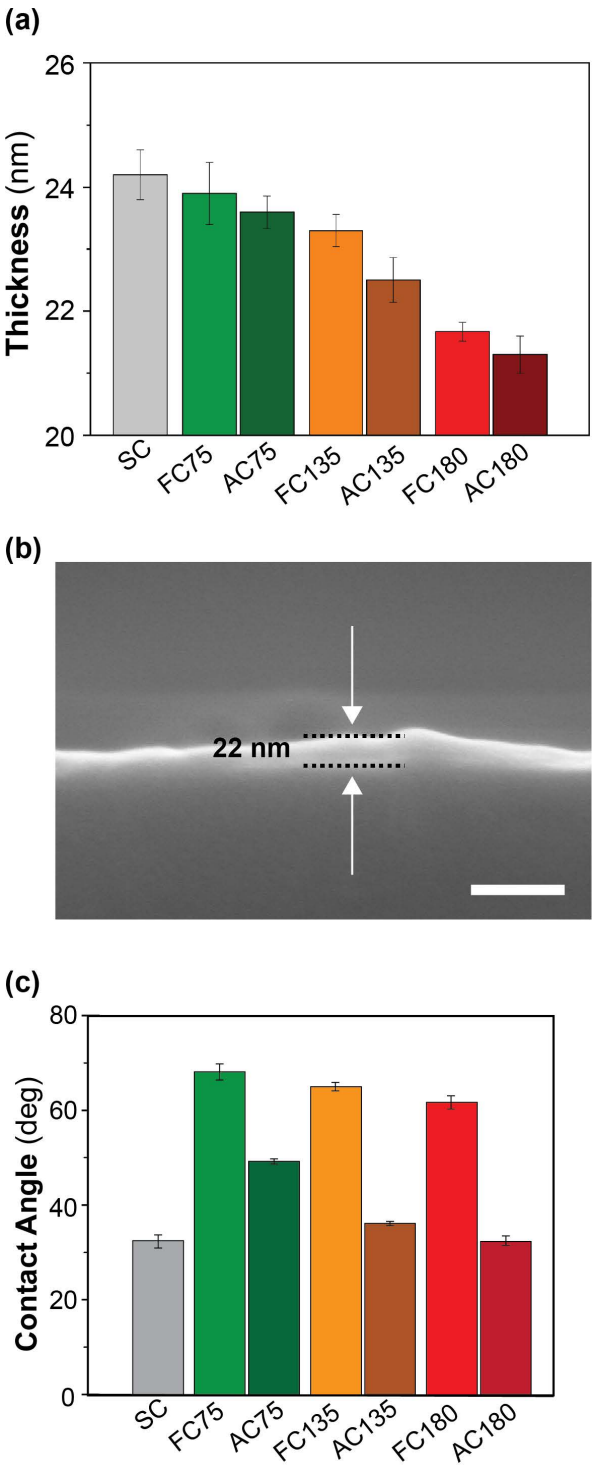

Figure 3. (a) Thickness of different coatings as measured by ellipsometry. Thickness decreases as temperature of treatment is increased, during both fluorous-curing as well as air-curing, due to tighter packing of collagen fibers (b) cross-section image of FC180 is in agreement with thickness measurements obtained through ellipsometry (c) Water contact angle measurement on treated and SC films using the static sessile drop method with 2 μL of water. PFHP treatment results in increased hydrophobicity as compared to treatment in air. Scale bar is 250 nm.

We next evaluated the stability of treated collagen films in aqueous media. Structural and mechanical properties of collagen-based materials are greatly affected by their tendency to swell in aqueous media, often resulting in a loss of structural features.[22] Based on the results in Figure 3, we expected samples treated at 180 °C to be resistant to swelling. Results from treatment conducted at other temperatures can be found in **Figure S4**. Samples were immersed in PBS for different time durations and the thickness of Col-I films were measured through ellipsometry, as seen in **Figure 4(a)**. After immersion for 24 h, the thickness of the SC film was reduced by ~50%. By comparison, only slight changes in thickness were observed in the case of FC180 and AC180. This demonstrates that heat treatment at 180° C improved significantly aqueous stability of collagen films. As duration of immersion is increased up to 4 days, FC180 continues to show no significant changes in thickness while AC180 shows significant *increase* in thickness, presumably due to swelling. This difference in stability suggests that collagen fibers are packed tighter post-PFHP treatment, as compared to air treatment. To further evaluate the difference between treatments in air and PFHP, nano-topographies of FC180 and AC180 after a 4-day immersion period were observed by AFM and shown in **Figures 4(b), (c)** (see also **Figure S3**). While the surface of FC180 **(Figure 4(b))** showed no significant changes post-immersion, the roughness of AC180 **(Figure 4(c))** sharply increased by ~2 nm. The morphology AC180 **(Figure 4(d))** observed by FESEM indicates the presence of a porous surface (nanopores and protuberances on the surface marked by the arrows) that may be responsible for the swelling. We hypothesized that the difference in the swelling behavior of FC180 and AC180 may be due to denaturation of collagen in the latter air-cured film. Collagen fibers heated in air are prone to denaturation and oxidation resulting in an amorphous polymer much like gelatin, which results in a higher degree of swelling as well as lower contact angles.[23]

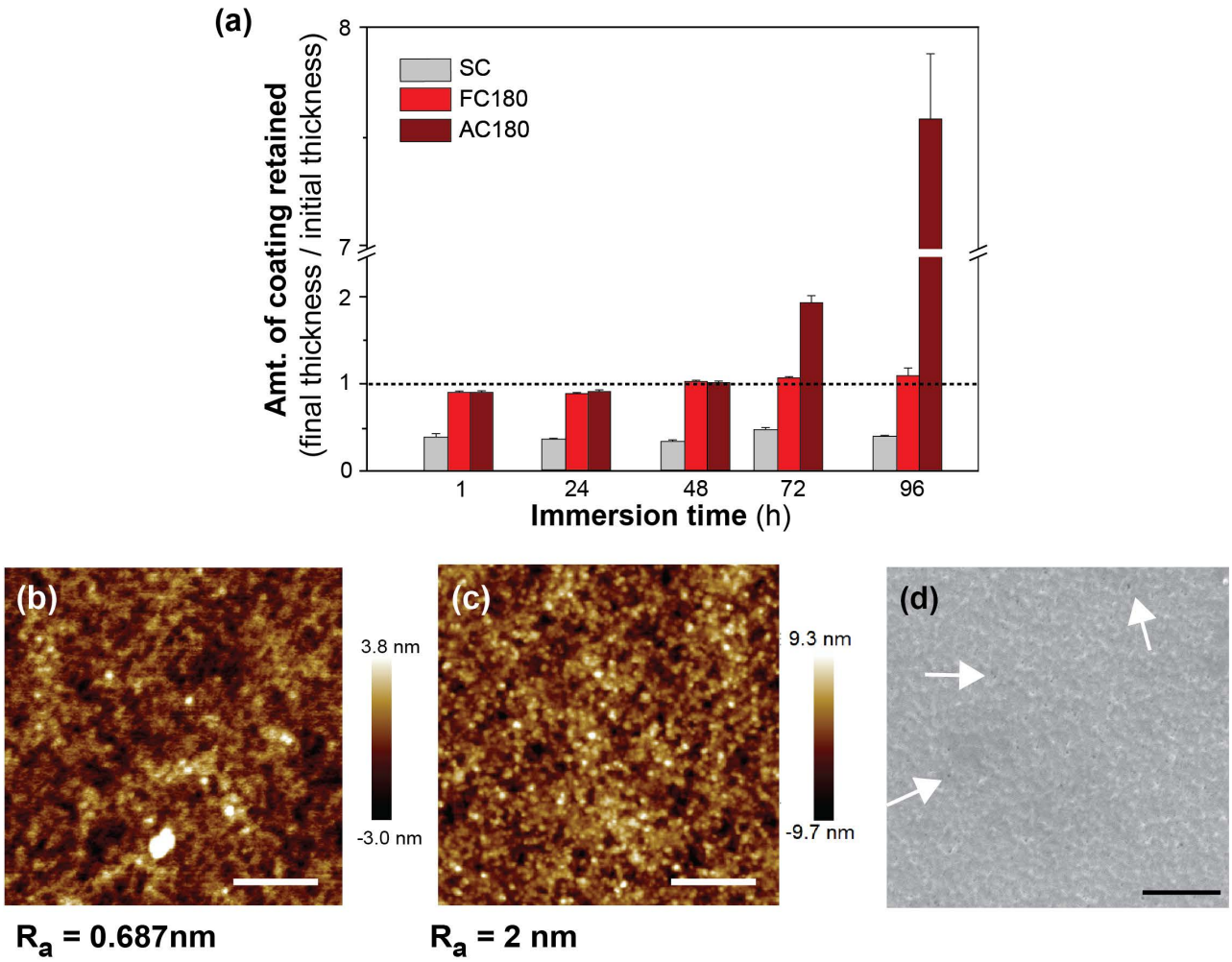

Figure 4. Stability of coatings in DPBS: (a) Thickness changes in coatings after immersion in PBS for different time durations. PFHP thermal treatment results in films less prone to swelling (b) and (c) nano-topographies of FC180 and AC180 after immersion in DPBS for 4 days, AC180 has significantly higher roughness compared to FC180. Average roughness calculated on the basis of two images per sample (d) surface morphology of AC180 immersed in PBS. Arrows indicate pores on the surface, which may contribute to increased swelling.

The structure of collagen I plays a key role in interaction with cells and dictates cell behavior such as alignment and phenotype. Based on the swelling studies in Figure 4(a), we hypothesized that the rapid increase in swelling of AC180 was most likely a result of significant denaturation and oxidation of collagen resulting in a gelatin-like[24] material. We evaluated the effect of thermal treatment on the structure of collagen-1 through ATR-FTIR and CD as shown in **Figure 5,** to assess the extent of denaturation. [25,26,27] The ATR-FTIR spectra of SC, FC180 and AC180 (**Figure 5(a)**) all exhibited absorption peaks of amide I (1700-1600 cm^{-1}, C=O stretching vibration), amide II ((1590-1500 cm^{-1},

N-H and C-N stretching vibration), 1454 cm^{-1} (bending vibration), 1300-1000 cm^{-1} (C-O stretching vibration), and amide III (1123, 1225cm^{-1}, the vibrations in C-N and N-H groups of bound amide). [25] The shape of amide I band is characteristic of the collagen secondary structure. Therefore, the Amide I (1700-1600 cm^{-1}) of SC, FC180 and AC180 were deconvoluted, transferred, baselined and resolved as shown in **Figure 5(b)**, according to established protocols. [25] The fitting of the band at 1660 cm^{-1} was assigned to prolyl carbonyls directed inside the triple helix (capable of intramolecular hydrogen bonding), and the band at 1630 cm^{-1} was assigned to the random coil form outwards in the triple helix. Thereafter, the calculated ratio of absorbance at 1660 and 1630 cm^{-1} was used to evaluate the denaturation of second structure of amide I. **Figure 5(c)** shows the area percentages of each band for different samples. Compared with SC, the ratio of α-helix/random coils decrease slightly for FC180, but strongly for AC180 **(Figure 5(c))**. The degree of denaturation, as calculated from **Figure 5(c)**, for AC180 and FC180are about 27% and 5% respectively with respect to SC. This indicated that PFHP treatment was able to resist heat-associated denaturation of collagen. This reduced denaturation was further confirmed by the CD spectra as shown in **Figure 5(d)**. SC, FC180 and AC180 were examined and compared with a 2 mg/ml Col-I. For SC and FC180, the rotatory maxima and minima are at 221 and 197 nm respectively, and crossover points (zero rotation) are at approximately 214 nm, which are consistent with the native collagen I solution. However, for AC180, the intensities of rotatory maxima and minima both decrease considerably as compared to SC, indicating significant denaturation.[28] CD spectra of samples incubated in PBS for 4 days post-treatment (**Figure S5**) also show a similar trend indicating that post-treatment, there is no change in the protein structure and the swelling behavior is solely a result of the denaturation of protein in the air-cured sample.

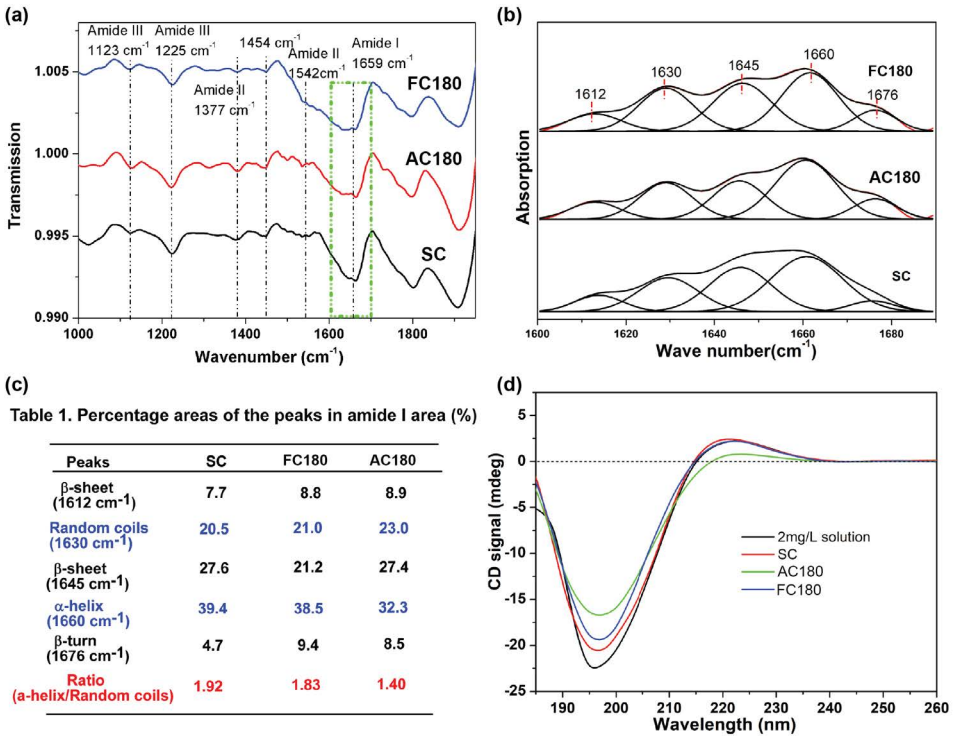

Peaks	SC	FC180	AC180
β-sheet (1612 cm-1)	7.7	8.8	8.9
Random coils (1630 cm-1)	20.5	21.0	23.0
β-sheet (1645 cm-1)	27.6	21.2	27.4
α-helix (1660 cm-1)	39.4	38.5	32.3
β-turn (1676 cm-1)	4.7	9.4	8.5
Ratio (a-helix/Random coils)	1.92	1.83	1.40

Figure 5. (a) Fourier-transform infrared spectra of SC, FC180 and AC180; (b) Amide I peak deconvolution of ß-sheet, random coils, α-helix and ß -turn contributes (red lines) elaborated by experimental curves for SC, FC180 and AC180; (c) Percentage areas of different peaks in amide I for SC, FC180 and AC180; (d) CD spectra of SC, FC180 and AC180 compared to Col-I solution. Results indicate significant denaturation of Col-I in the case of AC180.

Biomaterials are subjects to wear-and-tear during handling and within the body where mechanical failure can result in complications including delayed healing and chronic pain.[29] Improving the mechanical properties of collagen fibers is crucial for biomaterial applications, as mechanical failure is one of the major limitations of collagen-based materials.[30] Furthermore, the mechanical properties of the material must be tunable based on its intended application. For instance, tissue engineering scaffolds must mimic the mechanical properties of native tissue.[3132] Therefore, the ability to tune the mechanical properties of collagen films is important for designing novel biomaterials. We evaluated the mechanical properties of the fluorous-cured coatings by testing the cohesion strength, reduced modulus and hardness. The cohesion strength of the films was evaluated through sonication in aqueous

media. Treated and untreated films were sonicated in PBS for 5 and 25 min respectively and thickness before and after treatment was compared **(Figure 6(a))** (see also **Figure S6)**. As expected, films treated at 180°C remained stable after 25 min of ultrasound treatment. In contrast, the untreated spin-coated film showed low cohesion strength, with only 50% of the film retained after 5 min of ultrasonic treatment. The thickness of films treated at 75°C reduced by 20% after 5 min and by > 80% after 25 min **(S2).** These results further support our hypothesis that heat treatment induces tighter packing of collagen fibers, thereby increasing the stability and cohesion strength of films. Based on these results, the reduced modulus and hardness of SC, FC180 and AC180 were evaluated through nanoindentation. **Figure 6(b)** shows the load-displacement curves obtained through nanoindentation. With increased load, the indenter displaced significantly in the case of SC - ~100 nm during load maintaining and ~190 nm of residual displacement after unloading. This displacement indicates good plasticity of as-prepared Col-I. In contrast, the displacements for FC180 and AC180 decreased considerably (~ 50 nm during or after loading). The reduced modulus and hardness were calculated and tabulated in **Figure 6(c)**. A significant increase in reduced modulus and hardness was observed - ~10 times SC in the case of FC180. Additionally, XPS measurements **(Figure S7)** showed that no fluorine was incorporated into the film due to the treatment.

Collagen-based coatings are widely studied for wound-healing and tissue repair applications. However, rapid enzymatic digestion of coatings can lead to improper tissue repair due to lack of support for the growing tissue. Ideally, the scaffold should degrade at a rate proportional to the grown of new tissue.[33] For this reason, the ability to tune the rate of degradation of the collagen coating is crucial. We tested the enzymatic degradability of FC180, AC180 and SC by incubating them in trypsin solution for 5-120 min **(Figure 6(d))**. After 5 min incubation in trypsin, ~ 70% of the SC film was digested, while both heat-treated films remained relatively stable. However, as treatment was prolonged, marked differences in FC180 and AC180 was observed. After 120 min treatment, while

most of the SC and AC180 films were digested, ~30% of the FC180 film was retained. These results indicate that PFHP treatment significantly improved the enzymatic stability of collagen films as compared to untreated collagen films.

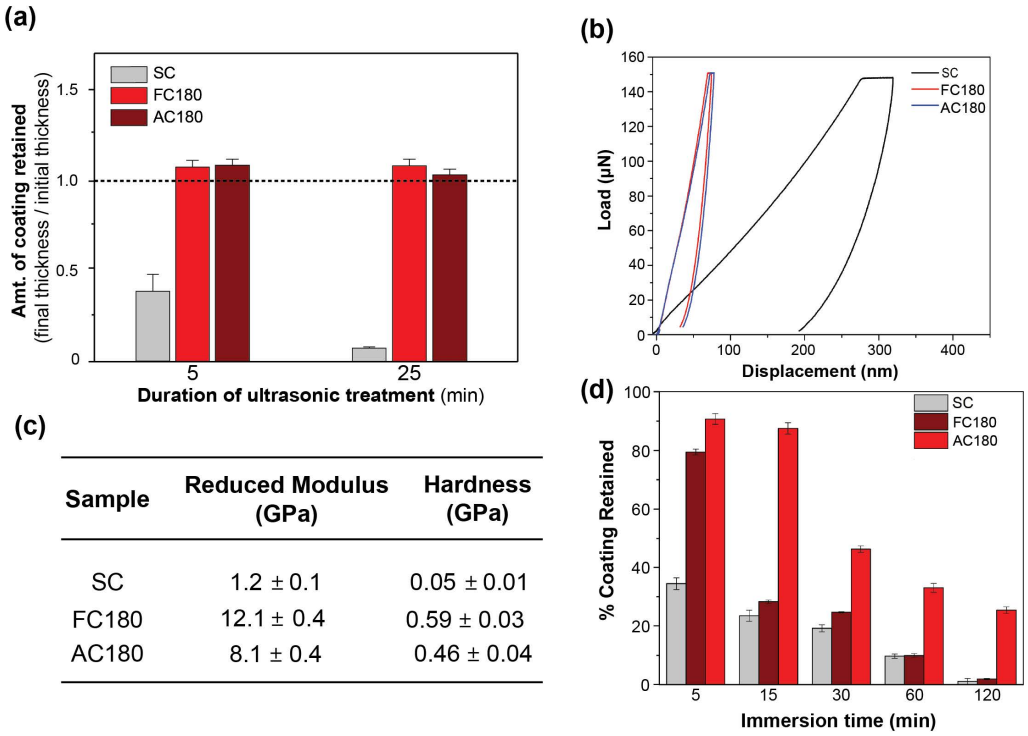

(c)

Sample	Reduced Modulus (GPa)	Hardness (GPa)
SC	1.2 ± 0.1	0.05 ± 0.01
FC180	12.1 ± 0.4	0.59 ± 0.03
AC180	8.1 ± 0.4	0.46 ± 0.04

Figure 6. (a) Thickness changes in coatings post ultrasonic treatment in PBS for different time durations. Treated films show greater cohesion strength. Scale bars are 1 μm. b) Load-displacement curves of SC, FC180 and AC180 recorded with increasing the applied load; (c) reduced modulus and hardness calculated and tabulated for SC, FC180 and AC180; PFHP treatment results in mechanically robust films (d) percentage of coatings retained post exposure to enzyme (0.025% trypsin solution) for different durations. PFHP treatment enhances enzymatic stability of collagen films.

Collagen coatings are widely applied as tissue engineering scaffolds due to their excellent cytocompatibility.[7,8] Surface properties such as chemical composition, nanotopography, and wettability dictate cell behavior such as adhesion, proliferation and differentiation.[34] We therefore evaluated the effect of the PFHP treatment on the cytocompatibility of collagen films by studying the behavior of mouse fibroblasts (L-929) to our treated collagen coatings. Cell adhesion and viability studies were performed on FC180, AC180, SC and bare Si **(Figure 7)**. There was no significant

statistical difference in the cell viability of the different coatings, according to the results obtained from the alamar Blue assay **(Figure 7(a))**. The % cell viability was calculated with respect to that of bare Si. The cell adhesion and morphology was evaluated through Live/Dead staining in the fluorescence images in **Figure 7(b)-(d)**. Most of the cells were live (stained green) indicating that all surfaces exhibited high cell viability. The adherent cells were mostly spherical on Si; larger spindle-like cells were observed on coated surfaces. We therefore concluded that PFHP treatment has no significant effect on the biocompatibility of collagen films.

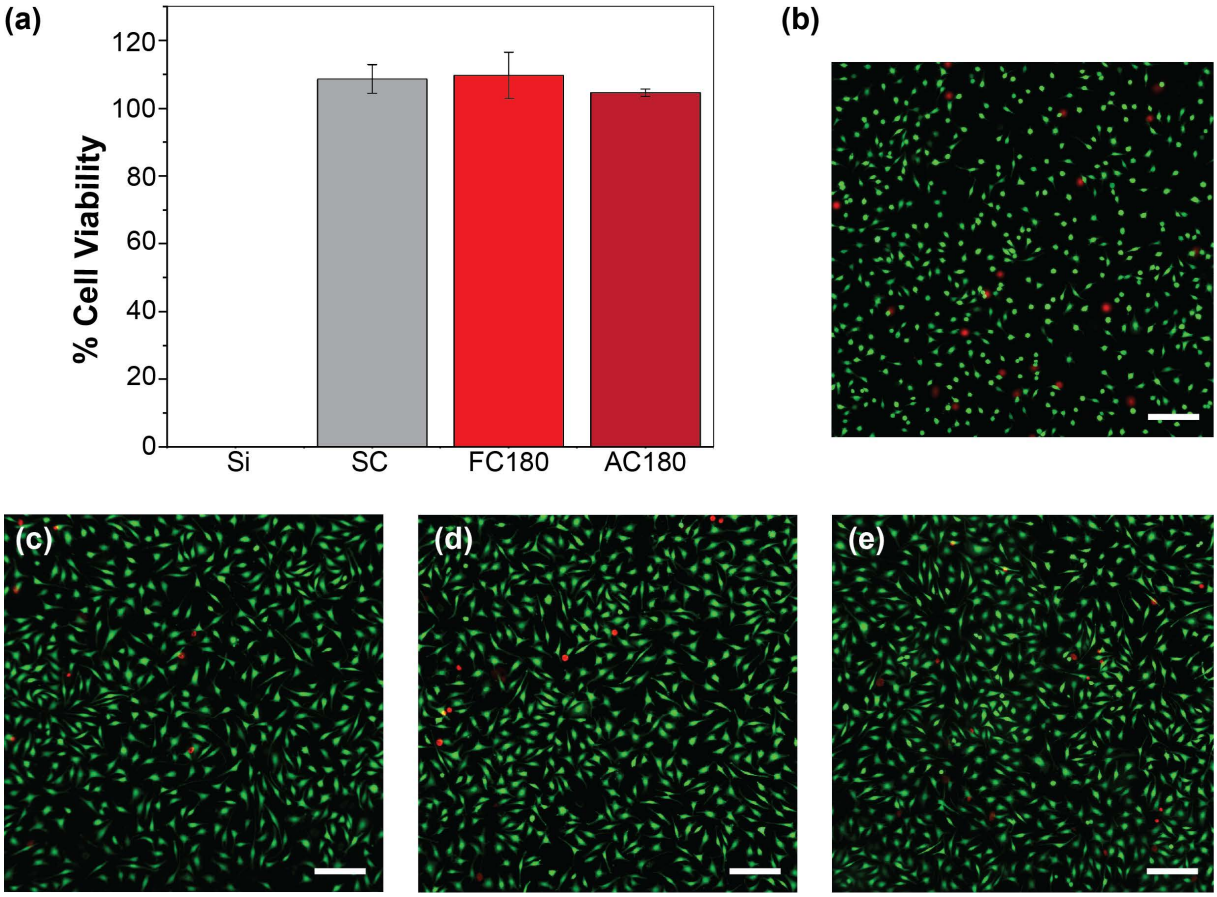

Figure 7. (a) % Cell viability of L-929 cells after incubation for 1d with respect to growth control (Bare Si), as determined by alamar Blue assay and (b) Live-dead staining of L-929 cells adhered on the surface of (b) Si, (c) SC, (d)FC180, (e) AC180 after 1d incubation time. No significant effect on viability observed post treatment. % cell viability was calculated with respect to bare Si. Scale bars are 200 μm.

CONCLUSION

This study discusses an approach for the fabrication of collagen-based materials utilizing a thermal treatment strategy in a fluorous-based solvent. We demonstrate our ability to enhance the stability relative to uncured or air-cured collagen films and our ability to tune the mechanical properties and enzymatic degradation solely by controlling the temperature of stabilization. Furthermore, the PFHP-based thermal treatment strategy can be successfully used strengthen and stabilize Col I-based biomaterials without compromising biocompatibility and native protein structure. This strategy provides an additive-free approach to design collagen-based biomaterials with improved mechanical and enzymatic stability.

MATERIALS AND METHODS

Fabrication of coatings

Silicon wafers (1cm×1cm, WRS Materials) were ultrasonically washed in ethanol and isopropanol for 10 min each and then treated with oxygen plasma (ITHCA, PDC-001, New York) at an oxygen pressure of 300 Pa for 5 min. A 3 mg/ml Col-I solution (A1048301, Thermo Fisher Scientific) was then spin-coated on cleaned Si wafer at 300 rpm for 50 s. The spin-coated samples were thermally treated in PFHP (perfluoroperhydrophenanthrene, procured from Sigma Aldrich) or air for 15 min at 75, 135 and 180 °C, respectively. Samples were then washed with perfluorohexane (Sigma Aldrich) to remove excess PFHP and dried with a stream N_2 gas. The as spin-coated samples were abbreviated as SC, the samples treated in PFHP solution as FC-T and the samples treated in air as AC-T, where T represents the temperature according to the treatment.

Structural characterization of coatings

The nano-topographies of the coatings were examined by atomic force microscopy (AFM, Bruker Dimension Icon) using Tapping Mode recorded at 2 kHz. The thickness of the coatings was measured by a Rudolph Research Auto EL ellipsometer (GAERTNER Scientific Corporation). Far-UV circular dichroism (CD) spectra were measured on a JASCO J-815 spectropolarimeter (Jasco UK, Essex, UK) with a quartz cuvette at 25 °C. The spectra were recorded from 185 to 260 nm with acetic acid (pH=4) at a rate of 10 nm/min. Attenuated total reflection micro-infrared（ATR-IR）spectra were recorded on a Bruker Vertex70 spectrometer at a spectral resolution of 4 cm^{-1}. The spectra of selected area were dealt with PeakFit4.12（SPSS Inc., Chicago, IL, USA to find the baseline, deconvolve Gaussian IRF, and resolve peaks.

The wettability of different surfaces was determined by measuring the water contact angle through the static sessile drop method (DSA30, Kruss, Germany). A 2.0 μL drop of milliQ water was dropped onto the substrate and an image was captured. The contact angle was then measured by the equipped analysis software (DSAI). This process was repeated thrice per sample to obtain a statistically relevant average.

Stability and mechanical characterization of the coatings

The cohesion strength of the collagen films was evaluated by ultrasonic treatment of the coatings in Dulbecco's Phosphate Buffered Saline (DPBS) at 60 Hz for 5 and 25 min. The samples were then gently rinsed with MilliQ water, dried with N_2, and the change in thickness was calculated through ellipsometry measurements.

The stability of collagen was evaluated by its degree of dissolution or swelling in PBS. Different samples were immersed in 1 ml PBS with or without 0.025% trypsin and incubated in an incubator at 37 °C with 5% CO_2 and 95% air for different times. After treatment for pre-determined times, the

samples were rinsed with MilliQ water, dried and the thickness change was evaluated as described above. Additionally, the morphologies of FC180 and AC180 after immersed in PBS for 4 days were observed by field emission scanning electron microscope (FESEM, SU6600, Hitachi, Japan) and AFM, respectively.

For the measurements of elastic modulus and hardness, TriboIndenter system (Hysitron TI 950, USA) with a 100 nm spherical indenter was used to perform nanoindentation. Thick Col-I coatings were prepared to minimize the influence of Si substrate on the elastic modulus and hardness measurements. Each Si wafer was carefully drop-casted with 100 μL Col-I solution, dried in vacuum, and then treated in PHFP or air at 180 °C for 15 min to fabricate a coating with thickness more than 500 nm. During each test, the load was increased up to 150 μN with a constant loading rate dP/dt=30 μN/s and kept for 3 s. Four tests were performed on each sample.

Cell adhesion evaluation

Cell culture

The fibroblast cells (L-929) were purchased from the Institute of Biochemistry and Cell Biology of Chinese Academy of Sciences (Shanghai, China).These cells were inoculated in modified Eagle's medium (MEM, Hyclone, USA) containing 10% fetal bovine serum (Hyclone, USA) and cultured at 37 °C with 5% CO_2. The media was refreshed every other day.

Cell viability assay

The coated Si substrates were placed in 24-well plates. 10^5 cells/ ml were seeded in each well and incubated for 24 h. Viability of fibroblast cells was assessed by the alamar Blue assay (protocol prescribed by the manufacturer-Thermo Fisher Scientific). Additionally, LIVE/DEAD staining was

performed using the LIVE/DEAD Viability/Cytotoxicity Kit (Invitrogen, France) as instructed by the manufacturer. The stained cells were observed using epifluorescence (SMZ745T, Nikon, Japan).

ASSOCIATED CONTENT

Supporting Information. Supporting information includes – Additional SEM, AFM and cross-sectional SEM images; Swelling behavior studies and cohesion strength characterization at different treatment temperatures; CD spectra for films after 4-day incubation in PBS; XPS characterization of film composition. Supporting information is available free of charge at https://pubs.acs.org/journal/aamick.

AUTHOR INFORMATION

CORRESPONDING AUTHOR

*Vincent M. Rotello

Department of Chemistry,

University of Massachusetts Amherst, MA, 01003, USA

Email – rotello@chem.umass.edu

*Yong Han

State-key Laboratory for Mechanical Behavior of Materials,

Xi'an Jiaotong University, Xi'an 710049, China

Email - yonghan@mail.xjtu.edu.cn

PRESENT ADDRESSES

†If an author's address is different than the one given in the affiliation line, this information may be included here.

AUTHOR CONTRIBUTIONS

The manuscript was written through contributions of all authors. All authors have given approval to the final version of the manuscript. ‡These authors contributed equally.

FUNDING SOURCES

Authors S.G., V.M.R., received funding from NSF (Center for Autonomous Chemistry CHE-1740597). Authors L.Z., K.L., and Y.H., received funding from National Natural Science Foundation of China (Grant number 51771142, 51571158, 51631007)) and National Key Research and Development Program of China No. 2016YFC1100600 (sub-project 2016YFC1100604).

ACKNOWLEDGEMENTS

We appreciate Research Fund for the NSF (Center for Autonomous Chemistry CHE-1740597), National Natural Science Foundation of China (Grant number 51771142, 51571158, 51631007)), National Key Research and Development Program of China No. 2016YFC1100600 (sub-project 2016YFC1100604) for financially supporting this work. We also acknowledge Danli Zhang for assistance with the nanoindentation experiment.

REFERENCES

1. Sorushanova, A.; Delgado, L. M.; Wu, Z.; Shologu, N.; Kshirsagar, A.; Raghunath, R.; Mullen, A. M.; Bayon, Y.; Pandit, A.; Raghunath, M.; Zeugolis, D.I. The Collagen Suprafamily: From Biosynthesis to Advanced Biomaterial Development. *Advanced Materials*. Wiley-VCH Verlag **2019**. https://doi.org/10.1002/adma.201801651.

2. Hosseinkhani, H.; Hiraoka, Y.; Li, C. H.; Chen, Y. R.; Yu, D. S.; Hong, P. Da; Ou, K. L. Engineering Three-Dimensional Collagen-IKVAV Matrix to Mimic Neural Microenvironment. *ACS Chem. Neurosci.* **2013**, *4* (8), 1229–1235. https://doi.org/10.1021/cn400075h.

3. karimizade, A.; takallu, sakine; Mirzaei, E. Evaluating the Effect of PH on Mechanical Strength and Cell Compatibility of Nanostructured Collagen Hydrogel by the Plastic Compression Method. *Nanomedicine J.* **2018**, *5* (3), 180–185. https://doi.org/10.22038/nmj.2018.005.0008.

4. Sun, L.; Li, B.; Yao, D.; Song, W.; Hou, H. Effects of Cross-Linking on Mechanical, Biological Properties and Biodegradation Behavior of Nile Tilapia Skin Collagen Sponge as a Biomedical Material. *J. Mech. Behav. Biomed. Mater.* **2018**, *80*, 51–58. https://doi.org/10.1016/j.jmbbm.2018.01.006.

5. Gautieri, A.; Vesentini, S.; Redaelli, A.; Buehler, M. J. Hierarchical Structure and Nanomechanics of Collagen Microfibrils from the Atomistic Scale Up. *Nano Lett.* **2011**, *11* (2), 757–766. https://doi.org/10.1021/nl103943u.

6. Tapeinos, C.; Larrañaga, A.; Sarasua, J. R.; Pandit, A. Functionalised Collagen Spheres Reduce H2O2 Mediated Apoptosis by Scavenging Overexpressed ROS. *Nanomedicine Nanotechnology, Biol. Med.* **2018**, *14* (7), 2397–2405. https://doi.org/10.1016/j.nano.2017.03.022.

7. Kaczmarek, B.; Sionkowska, A.; Gołyńska, M.; Polkowska, I.; Szponder, T.; Nehrbass, D.; Osyczka, A. M. In Vivo Study on Scaffolds Based on Chitosan, Collagen, and Hyaluronic Acid with Hydroxyapatite. *Int. J. Biol. Macromol.* **2018**, *118* (Pt A), 938–944. https://doi.org/10.1016/j.ijbiomac.2018.06.175.

8. Pettian, M. S.; Plepis, A.M.G.; Martins, V.D.C.A; Dos Santos, G.R..; Pinto, C.A.L.; Galdeano, E. A.; Calegari, A.R.A; de Moraes, C.A.; Cunha, M.R.D. Use of an Anionic Collagen Matrix Made from Bovine Intestinal Serosa for in Vivo Repair of Cranial Defects. **2018**. https://doi.org/10.1371/journal.pone.0197806.

9. Gaspar-Pintiliescu, A.; Seciu, A. M.; Miculescu, F.; Moldovan, L.; Ganea, E.; Craciunescu, O. Enhanced Extracellular Matrix Synthesis Using Collagen Dressings Loaded with Artemisia Absinthium Plant Extract. *J. Bioact. Compat. Polym.* **2018**, *33* (5), 516–528. https://doi.org/10.1177/0883911518783216.

10. Zhang, D.; Wu, X.; Chen, J.; Lin, K. The Development of Collagen Based Composite Scaffolds for Bone Regeneration. *Bioactive Materials*. KeAi Communications Co. March 1, 2018, pp 129–138. https://doi.org/10.1016/j.bioactmat.2017.08.004.

11. Ferreira, A. M.; Gentile, P.; Chiono, V.; Ciardelli, G. Ferreira, A. M., Gentile, P., Chiono, V., & Ciardelli, G. (2012). Collagen for Bone Tissue Regeneration. *Acta Biomater.* **2012**, *8* (9), 3191–3200. https://doi.org/10.1016/j.actbio.2012.06.014.

12. Ryan, A. J.; Kearney, C. J.; Shen, N.; Khan, U.; Kelly, A. G.; Probst, C.; Brauchle, E.; Biccai, S.; Garciarena, C. D.; Vega-Mayoral, V.; Loskill, P.; Kerrigan, S.W.; Schenke-Leyland, K.; Coleman, J.N.; O'Brien, F.J. Electroconductive Biohybrid Collagen/Pristine Graphene

Composite Biomaterials with Enhanced Biological Activity. *Adv. Mater.* **2018**, *30* (15), e1706442. https://doi.org/10.1002/adma.201706442.

13. Terzi, A.; Storelli, E.; Bettini, S.; Sibillano, T.; Altamura, D.; Salvatore, L.; Madaghiele, M.; Romano, A.; Siliqi, D.; Ladisa, M.; De Caro, L.; Quattrini, A.; Valli, L.; Sannino, A.; Giannini, C. Effects of Processing on Structural, Mechanical and Biological Properties of Collagen-Based Substrates for Regenerative Medicine. *Sci. Rep.* **2018**, *8* (1). https://doi.org/10.1038/s41598-018-19786-0.

14. Koide, M.; Osaki, K.; Konishi, J.; Oyamada, K.; Katakura, T.; Takahashi, A.; Yoshizato, K. A New Type of Biomaterial for Artificial Skin: Dehydrothermally Cross-Linked Composites of Fibrillar and Denatured Collagens. *J. Biomed. Mater. Res.* **1993**, *27* (1), 79–87. https://doi.org/10.1002/jbm.820270111.

15. Sionkowska, A.; Skopinska-Wisniewska, J.; Gawron, M.; Kozlowska, J.; Planecka, A. Chemical and Thermal Cross-Linking of Collagen and Elastin Hydrolysates. *Int. J. Biol. Macromol.* **2010**, *47* (4), 570–577. https://doi.org/10.1016/j.ijbiomac.2010.08.004.

16. Samouillan, V.; Delaunay, F.; Dandurand, J.; Merbahi, N.; Gardou, J.-P.; Yousfi, M.; Gandaglia, A.; Spina, M.; Lacabanne, C. The Use of Thermal Techniques for the Characterization and Selection of Natural Biomaterials. J. Funct. Biomater. 2011, 2 (3), 230–248. https://doi.org/10.3390/jfb2030230.

17. Zhu, D.-W. Perfluorocarbon Fluids: Universal Suspension Polymerization Media. *Macromolecules* **1996**, *29* (8), 2813–2817. https://doi.org/10.1021/ma951540x.

18. Marsh, E. N. G. Fluorinated Proteins: From Design and Synthesis to Structure and Stability. *Acc. Chem. Res.* **2014**, *47* (10), 2878–2886. https://doi.org/10.1021/ar500125m.

19. Asakura, T.; Adachi, K.; Schwartz, E. Stabilizing Effect of Various Organic Solvents on Protein. *J Bio. Chem.* **1978** 253, 6423-6423.

20. Uversky, V. N.; Narizhneva, N. V.; Kirschstein, S. O.; Winter, S.; Löber, G. Conformational Transitions Provoked by Organic Solvents in β-Lactoglobulin: Can a Molten Globule like Intermediate Be Induced by the Decrease in Dielectric Constant? Fold. Des. 1997, 2 (3), 163–172. https://doi.org/10.1016/S1359-0278(97)00023-0.

21. Wang, L. S.; Gopalakrishnan, S.; Lee, Y. W.; Zhu, J.; Nonnenmann, S. S.; Rotello, V. M. Translation of Protein Charge and Hydrophilicity to Materials Surface Properties Using Thermal Treatment in Fluorous Media. *Mater. Horizons* **2018**, *5* (2), 268–274. https://doi.org/10.1039/c7mh00933j.

22. Madaghiele M.; Calo E.; Salvatore L.; Bonfrate V.; Pedone D.; Frigione M.; Sannino A.; Assessment of collagen crosslinking and denaturation for the design of regenerative scaffolds. *J Biomed Mater Res Part A:* **2016** 104A: 186-194, https://doi.org/10.1002/jbm.a.35554.

23. Millington, K. R.; Ishii, H.; Maurdev, G. Chemiluminescence from Thermal Oxidation of Amino Acids and Proteins. *Amino Acids* **2010**, *38* (5), 1395–1405. https://doi.org/10.1007/s00726-009-0352-6.

24. Bozec, L.; Odlyha, M. Thermal Denaturation Studies of Collagen by Microthermal Analysis and Atomic Force Microscopy. Biophys. J. 2011, 101 (1), 228–236. https://doi.org/10.1016/j.bpj.2011.04.033.

25. Payne, K. J.; Veis, A. Fourier Transform Ir Spectroscopy of Collagen and Gelatin Solutions: Deconvolution of the Amide I Band for Conformational Studies. *Biopolymers* **1988**, *27* (11), 1749–1760. https://doi.org/10.1002/bip.360271105.

26. Silva, Z. S.; Botta, S. B.; Ana, P. A.; França, C. M.; Fernandes, K. P. S.; Mesquita-Ferrari, R. A.; Deana, A.; Bussadori, S. K. Effect of Papain-Based Gel on Type I Collagen - Spectroscopy Applied for Microstructural Analysis. *Sci. Rep.* **2015**, *5*. https://doi.org/10.1038/srep11448.

27. De Campos Vidal, B.; Mello, M. L. S. Collagen Type I Amide I Band Infrared Spectroscopy. *Micron* **2011**, *42* (3), 283–289. https://doi.org/10.1016/j.micron.2010.09.010.

28. Kandamchira, A.; Selvam, S.; Marimuthu, N.; Janardhanan, S. K.; Fathima, N. N. Influence of Functionalized Nanoparticles on Conformational Stability of Type I Collagen for Possible Biomedical Applications. *Mater. Sci. Eng. C. Mater. Biol. Appl.* **2013**, *33* (8), 4985–4988. https://doi.org/10.1016/j.msec.2013.08.018.

29. Prasad, K.; Bazaka, O.; Chua, M.; Rochford, M.; Fedrick, L.; Spoor, J.; Symes, R.; Tieppo, M.; Collins, C.; Cao, A.; Markwell, D.; Ostrikov, K.K.; Bazaka, K. Metallic Biomaterials: Current Challenges and Opportunities. *Materials*. MDPI AG July 31, 2017. https://doi.org/10.3390/ma10080884.

30. Meyer, M. Processing of Collagen Based Biomaterials and the Resulting Materials Properties. *Biomed. Eng. Online* **2019**, *18* (1). https://doi.org/10.1186/s12938-019-0647-0.

31. Akhmanova, M.; Osidak, E.; Domogatsky, S.; Rodin, S.; Domogatskaya, A. Physical, Spatial, and Molecular Aspects of Extracellular Matrix of in Vivo Niches and Artificial Scaffolds Relevant to Stem Cells Research. Stem Cells Int. 2015, 2015. https://doi.org/10.1155/2015/167025.

32. Guarino, V.; Raucci, M. G.; Ronca, A.; Cirillo, V.; Ambrosio, L. Multifunctional Scaffolds for Bone Regeneration. In Bone Substitute Biomaterials; Elsevier Inc., 2014; pp 95–117. https://doi.org/10.1533/9780857099037.2.95.

33. Zhang, L.; Liu, X.; Li, G.; Wang, P.; Yang, Y. Tailoring Degradation Rates of Silk Fibroin Scaffolds for Tissue Engineering. J. Biomed. Mater. Res. Part A 2019, 107 (1), 104–113. https://doi.org/10.1002/jbm.a.36537.

34. Richbourg, N. R.; Peppas, N. A.; Sikavitsas, V. I. Tuning the Biomimetic Behavior of Scaffolds for Regenerative Medicine through Surface Modifications. *Journal of Tissue Engineering and Regenerative Medicine*. John Wiley and Sons Ltd 2019. https://doi.org/10.1002/term.2859.